RSC Advances

PAPER

View Article Online
View Journal | View Issue

Cite this: *RSC Adv.*, 2023, **13**, 30391

Asymmetric synthesis of chiral (thio)chromanes and exploration on their structure–activity relationship in macrophages†

Xiao Zhang,‡[ab] Qian Zhou,‡[c] Yue Zhou,[c] Zihao Wang,*[ef] Jun Wang[bd] and Mingfu Wang*[ac]

A CuCl/(*R*,*R*)-Ph-BPE-catalyzed enantioselective hydroallylation of 2*H*-chromenes and 2*H*-thiochromenes with allylic phosphate electrophiles is developed, which enables highly efficient and atom-economical asymmetric access to a series of 4-allyl chromanes and thiochromanes in high yields (up to 91%) with excellent enantioselectivities (up to 99% ee). These valuable chiral chromane and thiochromane products can serve as crucial intermediates for accessing bioactive compounds containing oxygen and sulfur atoms. In addition, the antioxidant and anti-inflammatory effects of various chromanes and thiochromanes were investigated in RAW 264.7 macrophages. The chromanes and thiochromanes exhibited significant inhibitory effects on the production of reactive oxygen species (ROS) and the secretion of pro-inflammatory cytokines, including interleukin-6 (IL-6) and tumor necrosis factor-α (TNF-α). These findings indicate that the newly synthesized chromanes and thiochromanes hold promise as potential lead compounds for the development of antioxidant and anti-inflammatory drugs.

Received 21st September 2023
Accepted 5th October 2023

DOI: 10.1039/d3ra06428j

rsc.li/rsc-advances

1. Introduction

Chiral chromanes represent a highly significant class of heterocyclic compounds characterized by a benzopyran hexagonal ring as the core structure. They are extensively encountered in natural products and pharmaceutical compounds, exhibiting appreciable biological activities[1] (Fig. 1(a)). For example, vitamin E (α-tocopherol) is a naturally occurring lipophilic antioxidant that acts as a scavenger for free radicals.[2] Catechin not only inhibits the formation of intestinal tumors and the activation of focal adhesion kinase,[3] but also inhibits atherosclerotic plaques in animal models.[4] Calanolide A prevents HIV-1 reverse transcriptase.[5] Cromankalim is a drug for the treatment of hypertension.[6] Centchroman[7] and Equol[8] are estrogen antagonists with antifertility properties. Because of that, the development and synthesis of chiral chromanes are of great significance. The asymmetric synthesis can reasonably modify the chiral sites according to the structure–activity relationship, which lays the groundwork for the following contents. By selectively modifying the chiral centers, researchers can fine-tune the properties and activities of the compound, aiming to optimize its pharmacological effects. Of note, the asymmetric synthesis of chiral chromanes has consistently been an area of interest for both organic synthesis and pharmaceutical applications.

Many transitions metal asymmetric methods for the synthesis of chiral chromanes[9–23] offer convenient access to desirable chromanes with complex structures and pharmacological activities in the past decades. The transition-metal catalyzed enantioselective functionalization of the C=C bond in 2*H*-chromene has been proved to be a direct and effective method for obtaining chiral chromanes. For instance, Hoveyda,[24] Hou,[25] and our group[26] realized copper (Cu)-catalyzed asymmetric hydroboration of 2*H*-chromenes in 2009, 2019 and 2022, respectively. In 2020 and 2021, our group[27,28] reported copper (Cu)-catalyzed asymmetric hydroamination of 2*H*-chromenes with *N*,*N*-dibenzylhydroxylamine ester (Fig. 1(b)-(a)). In 2017, Toste[9] disclosed palladium (Pd)-catalyzed enantioselective 1,3-arylfluorination of *ortho*-carb-oxamidesubstituted 2*H*-chromenes with arylboronic acids and selectfluor (Fig. 1(b)-(b)). In 2017, Zhang[29] described iridium (Ir)-catalyzed enantioselective hydrogenation for constructing chiral chromanes (Fig. 1(b)-(c)). In 2019, our group[30] and Nishimura[31]

[a]*School of Biological Science, The University of Hong Kong, Hong Kong 999077, China. E-mail: mfwang@hku.hk*

[b]*Department of Chemistry, Southern University of Science and Technology, Shenzhen 518055, China*

[c]*Shenzhen Key Laboratory of Food Nutrition and Health, Institute for Advanced Study, Shenzhen University, Shenzhen 518060, China*

[d]*Department of Chemistry, Hong Kong Baptist University, Hong Kong 999077, China*

[e]*School of Chinese Medicine, Hong Kong Baptist University, Hong Kong 999077, China. E-mail: wangzh21@hkbu.edu.hk*

[f]*Centre for Chinese Herbal Medicine Drug Development, Hong Kong Baptist University, Hong Kong 999077, China*

† Electronic supplementary information (ESI) available. CCDC 2296186. For ESI and crystallographic data in CIF or other electronic format see DOI: https://doi.org/10.1039/d3ra06428j

‡ The two authors contributed evenly to this work.

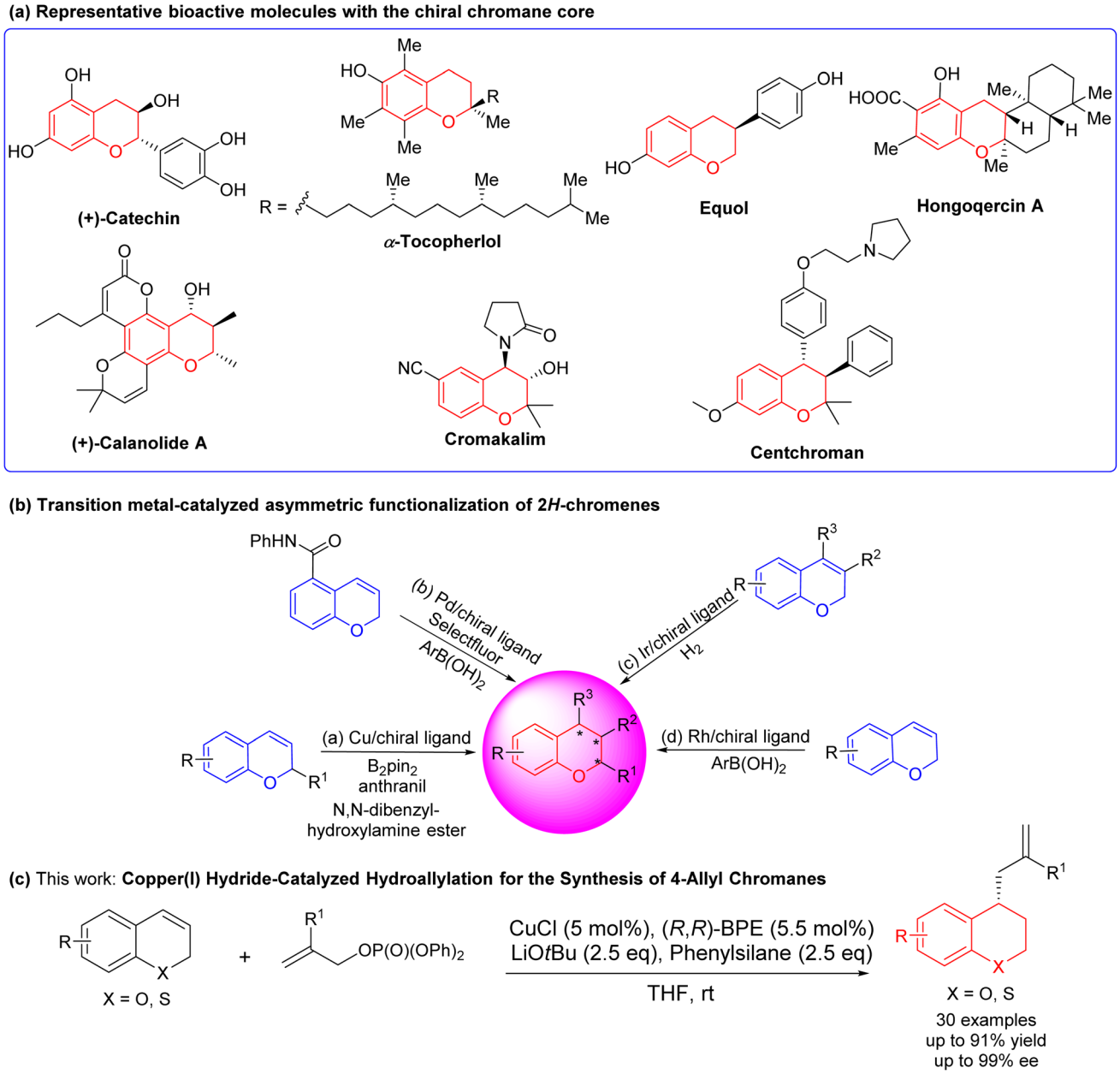

Fig. 1 Representative bioactive molecules with chiral chromane core and asymmetric synthesis of chromanes. (a) Representative bioactive molecules with the chiral chromane core. (b) Transition metal-catalyzed asymmetric functionalization of 2*H*-chromenes. (c) Copper(I) hydride-catalyzed hydroallylation for the synthesis of 4-allyl (thio)chromanes.

presented rhodium (Rh)-catalyzed asymmetric hydroarylation of 2*H*-chromenes (Fig. 1(b)-(d)). However, the current situation presents ongoing challenges including a restricted reaction type, limited generality, suboptimal product yields, and compromised enantioselectivity. And there is a strong motivation to invest in the development of direct asymmetric functionalization methods for 2*H*-chromenes, aiming to achieve the synthesis of enantio-enriched 4-allylchromanes. Buchwald,[32] Yun[33] and Hoveyda[34] pioneeringly illustrated copper hydride-catalyzed enantioselective hydroallylation for the synthesis of chiral allyl derivatives. This protocol offers several notable features, including mild reaction conditions, excellent tolerance towards various functional groups, and stereoselectivity. Later, Cu-catalyzed asymmetric hydroallylation has been applied to 1,2-dihydroquinolines by You in 2020.[35] However, there is no hydroallylation of 2*H*-chromenes and 2*H*-thiochromenes reported.

Building upon our ongoing progress in the synthesis of chiral bioactive flavonoids and thioflavonoids,[26–28,30,36–41] here, we reported a CuCl/(*R*,*R*)-Ph-BPE-catalyzed asymmetric hydroallylation of 2*H*-chromenes and 2*H*-thiochromenes to synthesize 4-allyl-substituted chromanes and thiochromanes (Fig. 1(c)). Moreover, biological investigations of these diversified 4-allyl chromanes were conducted by using

a lipopolysaccharide (LPS)-induced RAW 264.7 cell. While inflammation is an essential biological process triggered in response to various stimuli, including tissue injury, microbial pathogen infection, and chemical irritation.[42] Excessive inflammation is considered to be a critical factor in many human diseases and conditions, including obesity, cardiovascular diseases, neurodegenerative diseases, diabetes, aging, and cancer.[43] Epidemiological studies[44,45] have suggested an inverse correlation between the consumption of flavonoid-rich fruits and vegetables and the incidence of chronic diseases and cancer, possibly owing to the potential anti-inflammatory activities associated with these bioactive compounds. In particular, these newly synthesized chromanes were able to prevent LPS-induced oxidative stress and inflammation response at a non-toxic level to the cells. Also, structural activity relationship was analyzed to offer a practical understanding for future pharmacological synthesis in this field.

2. Materials and methods

2.1. Chemicals and materials

All the air- or moisture-sensitive reactions and manipulations were performed under an atmosphere of argon by using standard Schlenk techniques and Drybox (Mikrouna, Supper 1220/750). ^{1}H nuclear magnetic resonance (NMR) and ^{13}C NMR spectra were recorded on a 400 or 500 MHz Bruker Avance spectrometer. $CDCl_3$ was used as solvent. Chemical shifts (δ) were reported in parts per million with tetramethylsilane as the internal standard, and J values were given in hertz. The following abbreviations were used to explain the multiplicities: s, singlet; d, doublet; dd, double of doublets; t, triplet; q, quartet; m, multiplet. Flash column chromatograph was carried out using 200- to 300-mesh silica gel at medium pressure. High-resolution mass spectra (HRMS) were recorded on a liquid chromatography (LC)-time-of-flight spectrometer. Electrospray ionization (ESI)-HRMS data were acquired using a Thermo LTQ Orbitrap XL Instrument equipped with an ESI source. High-performance LC (HPLC) analysis was performed on Agilent 1260 series, and ultraviolet detection was monitored at 230 or 220 nm. Tetrahydrofuran was distilled over sodium.

Dulbecco's modified Eagle's medium including nutrient mixture (DMEM), fetal bovine serum (FBS), and antibiotic-antimycotic were obtained from Gibco (Gaithersburg, MD, USA). Phosphate buffered saline (PBS), and sodium bicarbonate were from Sigma (St. Louis, MO, USA). Cell counting kit-8 (CCK-8) and reactive oxygen species (ROS) assay kit were obtained from Beyotime (Shanghai, China). Enzyme-linked immunosorbent (ELISA) kits were purchased from Jonln Co. Ltd (Shanghai, China). Lipopolysaccharides (LPS) was obtained from Sigma (St. Louis, MO, USA).

2.2. Copper(I) hydride-catalyzed hydroallylation

The specific operation of copper(I) hydride-catalyzed hydroallylation was as follows: CuCl (0.01 mmol, 1.0 mg), **L1** (0.011 mmol, 5.6 mg) and THF (0.5 mL) were added into the reaction tube (10.0 mL) in a glove box filled with argon atmosphere. After stirring for 10 min at room temperature, phenylsilane (0.5 mol) was added, followed by stirring for 10 min at room temperature, followed by allyl phosphate (0.5 mmol), LiO*t*Bu (0.5 mmol, 40.0 mg), and chromene (0.2 mmol). The reaction tube was removed from the glove box and stirred at rt for 24 h. At the end of the reaction, the reaction was filtered through the funnel with EA and concentrated *in vacuo* and the residue was purified by silica gel column chromatography (PE) to provide chromane compound. The ee value of the product was determined by HPLC. Diastereomeric ratio was determined by ^{1}H NMR.

2.3. Cell culture

The RAW 264.7 cells were purchased from ATCC (Manassas, VA, United States). They were cultured in DMEM medium supplemented with 10% FBS and 1% antibiotic–antimycotic. The cells were maintained at 37 °C in a humidified incubator with 5% CO_2 and the medium was changed every other day. All cell experiments were conducted in RAW 264.7 cells within passage 30. For cytotoxicity studies, RAW 264.7 cells were treated with chromanes at indicated concentrations for 24 h. For ROS studies, RAW 264.7 cells treated with chromanes at indicated concentrations for 24 h and with LPS for 4 h, then incubated with 2′,7′-dichlorofluorescin diacetate (DCFH-DA) in a 37 °C incubator in the dark for 30 min.

2.4. Cell viability assay

To evaluate the cytotoxicity of the newly synthesized 4-allyl chromanes, cells were seeded into 96-well plates at the density of 10^5. After overnight, cells were treated with each test compound at different concentrations (0–200 μM) for 24 h. A commercial CCK-8 kit was used to detect their cytotoxicity by following the manufacturer's instructions. The data were calculated and expressed as percentage cell viability.

2.5. Detection of ROS

The intracellular level of ROS was assessed using a DCFH-DA fluorescent probe. After the treatment, cells were harvested and incubated with DCFH-DA in a 37 °C incubator in the dark for 30 min. At the end of incubation, the cells were washed with PBS three times and the fluorescence intensity of 2′,7′-dichlorodihydrofluorescein (DCF), which reflected the intracellular level of ROS, was analyzed by a Cell Imaging Multi-Mode Reader, BioTex Cytation 1.

2.6. Detection of inflammatory cytokines

RAW 264.7 cells were treated with these synthesized newly synthesized 4-allyl chromanes (25, 50 and 100 μM) for 24 hours followed by LPS (1 μg mL^{-1}) stimulation for another 4 hours, and the culture supernatant was collected. The concentrations of IL-6 and TNF-α in the culture supernatant of RAW 264.7 cells were determined according to the manufacturer's instructions of the ELISA kits, purchased from Jonln Co. Ltd (Shanghai, China).

2.7. Statistical analysis

Data from three independent experiments are presented as mean ± SD by GraphPad Prism 7.0 (GraphPad Software, San Diego, CA, USA). Student's two-tailed *t*-test was applied in comparing two groups, while one-way ANOVA followed by a Tukey's test was utilized in multiple comparisons. For all statistical tests, p value < 0.05 was considered statistically significant.

3. Results and discussion

3.1. Reaction condition optimization

We started the study by choosing chromene **1a** as the substrate. After treatment of **1a** (1 equiv.) with **2a** (2.5 equiv.) and DMMS (dimethoxymethylsilane, 2.5 equiv.) in the presence of CuCl catalyst (5 mol%) and (*R*,*R*)-Ph-BPE (5.5 mol%) in THF (1 M) at rt, the desired product **3aa** was isolated in 70% yield and 99% ee with Li*O*t*Bu (2.5 equiv.) as the base (entry 1, Table 1). Inspired by the results, we performed further optimization of the reaction conditions. Screening of different ligands (entries 1–6) revealed that (*R*,*R*)-Ph-BPE (**L1**) was the best ligand in this reaction (entry 1, Table 1). Screening of different silanes (entries 7–10, Table 1) revealed that phenylsilane gave the desired product **3aa** with 91% yield and 99% ee (entry 8, Table 1) in this reaction. Screening of different solvents (entries 11–13, Table 1) showed that THF gave the desired product **3aa** with 91% yield and 99% ee (entry 8, Table 1). Screening of different copper resources (entries 14–16, Table 1) showed that CuCl gave the desired product **3aa** with 91% yield and 99% ee (entry 8, Table 1). Thus, the following optimized reaction conditions were identified: **1a** (1 equiv.), **2a** (2.5 equiv.), phenylsilane (2.5 equiv.), CuCl (5 mol%), (*R*,*R*)-Ph-BPE (**L1**) (5.5 mol%), Li*O*t*Bu (2.5 equiv.) at rt for 24 h (entry 8, Table 1).

3.2. Substrate scope of 4-allyl chromanes

Next, the scope of substrates was explored under the optimal conditions mentioned above (Table 2). A series of substituents

Table 1 Optimization of reaction condition[a]

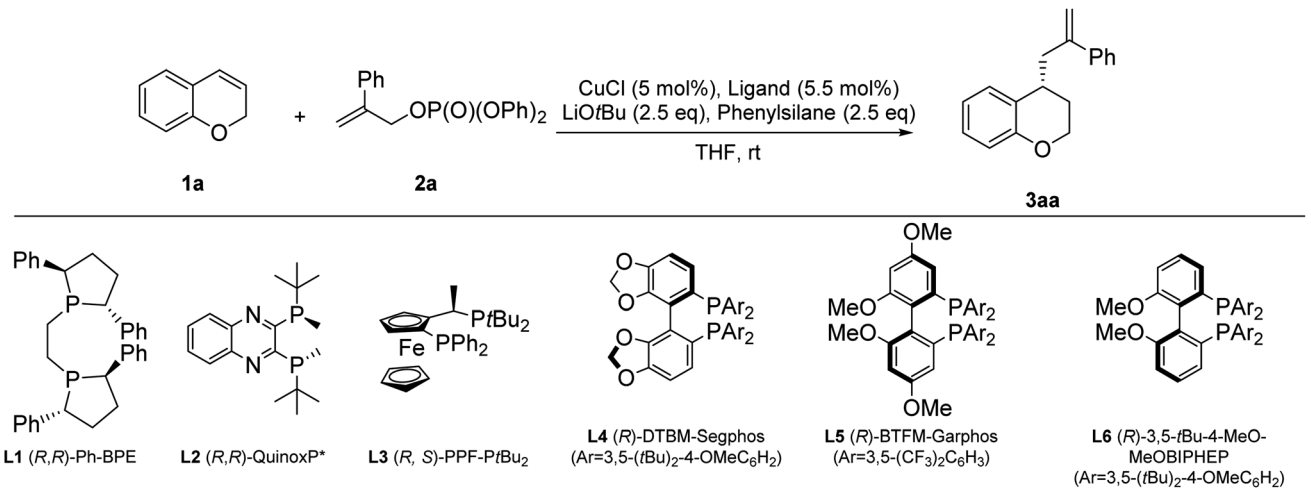

Entry	Ligand	Silane	Solvent	Copper resource	**3aa** yield[b] (%)	**3aa** ee[c] (%)
1	**L1**	DMMS	THF	CuCl	70	99
2	**L2**	DMMS	THF	CuCl	14	54
3	**L3**	DMMS	THF	CuCl	34	90
4	**L4**	DMMS	THF	CuCl	14	74
5	**L5**	DMMS	THF	CuCl	10	66
6	**L6**	DMMS	THF	CuCl	20	93
7	**L1**	DEMS	THF	CuCl	83	99
8	**L1**	Phenylsilane	THF	CuCl	91	99
9	**L1**	Diphenylsilane	THF	CuCl	90	99
10	**L1**	Trimethoxysilane	THF	CuCl	80	99
11	**L1**	Phenylsilane	DCM	CuCl	62	99
12	**L1**	Phenylsilane	Toluene	CuCl	57	99
13	**L1**	Phenylsilane	1,4-Dioxane	CuCl	64	99
14	**L1**	Phenylsilane	THF	$CuCl_2$	70	99
15	**L1**	Phenylsilane	THF	CuBr	66	99
16	**L1**	Phenylsilane	THF	CuI	60	99

[a] Reaction conditions: to a solution of copper sources (0.010 mmol, 5 mol%), **L1** (0.011 mmol, 5.5 mol%), Li*O*t*Bu (0.5 mmol, 2.5 equiv.) and phenylsilane (0.5 mmol, 2.5 equiv.) in 0.5 mL THF were added **1a** (0.2 mmol, 1 equiv.) and **2a** (0.5 mmol, 2.5 equiv.) in sequence. Catalyst was pre-prepared by mixing CuCl and **L1** together in THF at room temperature. The reaction mixtures were stirred at rt for 24 h. [b] Isolated yield. [c] Determined by HPLC analysis.

Table 2 Substrate scope

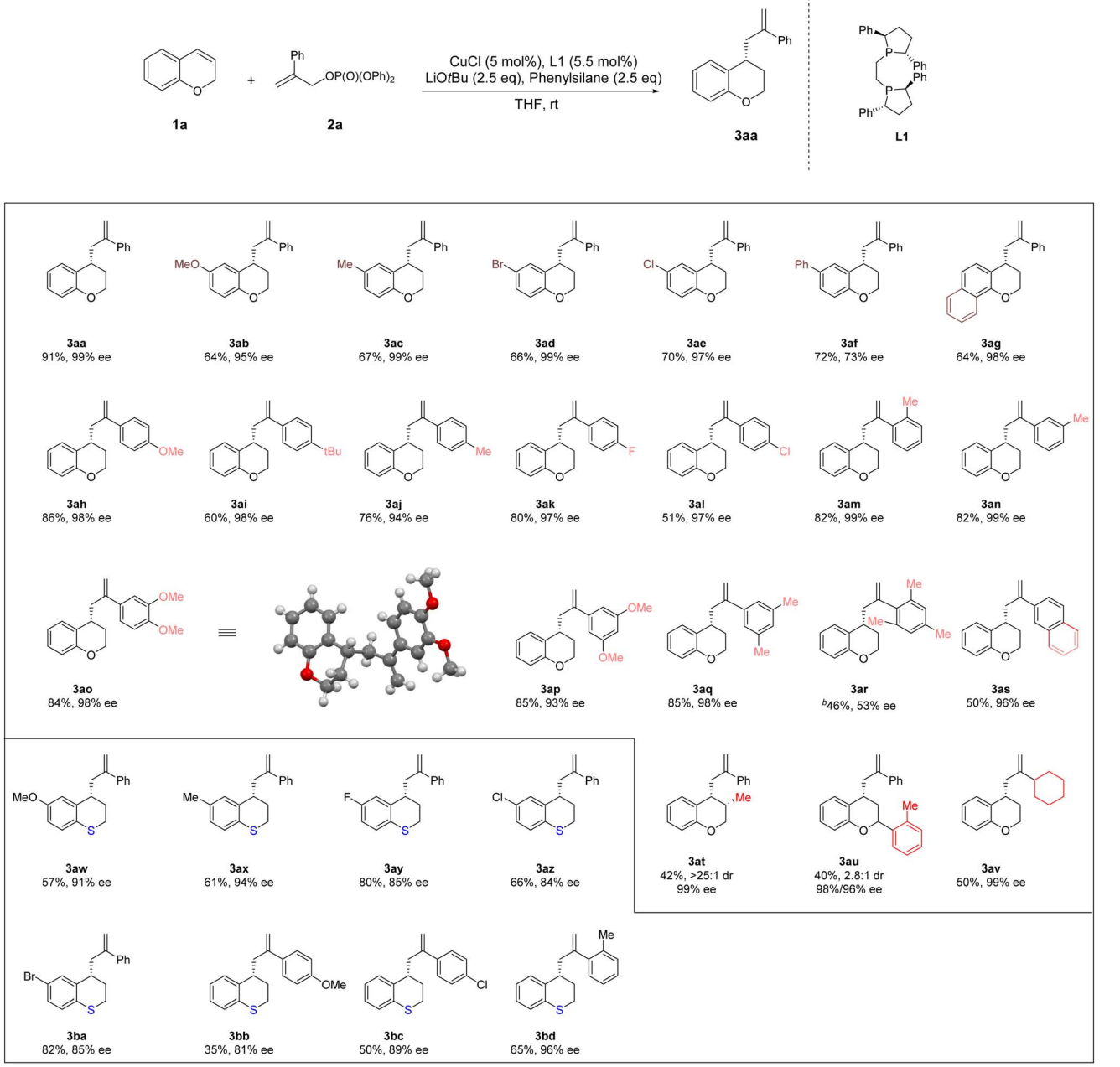

ranging from electron-donating groups (–Me and –OMe) to electron-withdrawing groups (–Br, –Cl, and –Ph) at C6 position of chromanes could be tolerated well (64–72% yield, 73–99% ee, **3ab**, **3ac**, **3ad** and **3af**). In addition, 7,8-substituted (*R*)-4-(2-phenylallyl)-chromane **3ag** was obtained in 64% yield and 98% ee. The 2- and 3-substituted chromanes could be transformed smoothly, furnishing **3au** and **3at** in moderate yields and moderate to good dr with excellent enantioselectivity (40–42% yield, 2.8 : 1 → 25 : 1 dr, 96–99% ee). Various allylic phosphates bearing both aryl and cyclohexylgroups at position 2 were accommodated, further broadening the substrate scope (46–86% yields, 53–99% ee, **3ah–3av**). A series of substituents ranging from electron-donating groups (–Me and –OMe) to electron-withdrawing groups (–F, –Br and –Cl) at C6 position of thiochromanes could be tolerated well (57–82% yield, 84–94% ee, **3aw–3az** and **3ba**). Various allylic phosphates bearing aryl groups at position 2 were accommodated in thiochromanes, further broadening the substrate scope (35–65% yield, 81–96% ee, **3bb–3bd**).

3.3. Synthetic application

To demonstrate the broad potential applicability of the methodology developed herein, we have successfully transformed the resulting chromane **3ad** into a highly valuable chiral intermediate **3be** *via* a coupling reaction with ethynyltriisopropylsilane in 40% yield and 99% ee. Furthermore, by subjecting the

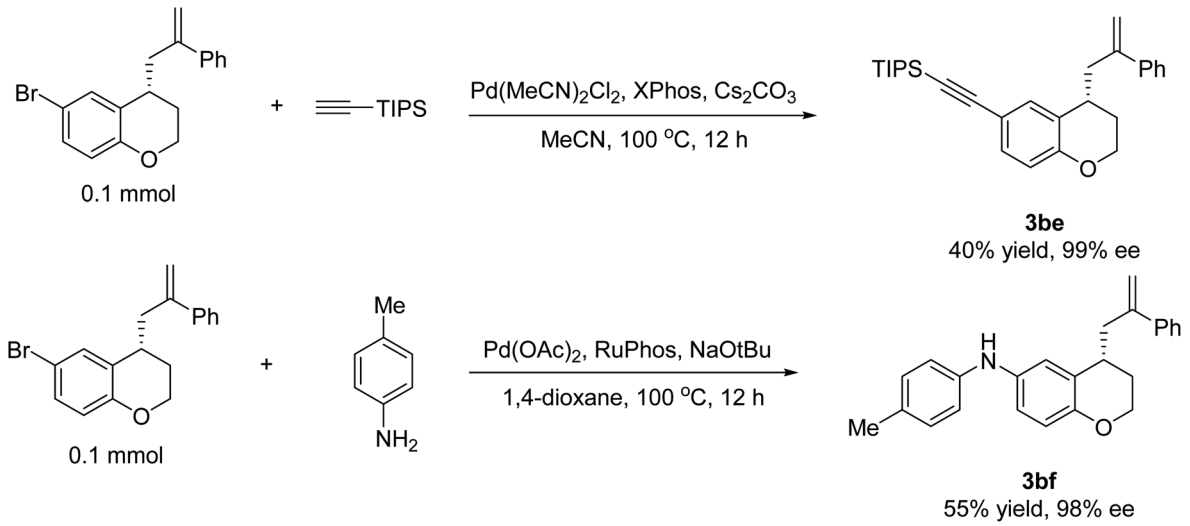

Fig. 2 Synthetic application.

chromane **3ad** to a coupling reaction with *p*-toluidine, we have also obtained **3bf** in 55% yield and 98% ee. These remarkable results not only show the versatility and utility of the developed synthetic methodology, but also highlight the potential of these chiral 4-allyl chromane derivatives as valuable building blocks for the preparation of novel compounds with potential applications in various fields, including drug discovery, materials science, and chemical biology (Fig. 2).

3.4. Cytotoxicity of 4-allyl chromanes

CCK-8 assay was performed to investigate the cytotoxicity of 4-allyl chromane and thiochromane compounds on RAW 264.7 cells (Fig. 3(a) and (b)). To further understand their structure–cytotoxicity relationship, the newly synthesized template compound **3aa** was applied as the model compound and IC_{50} of these 4-allyl chromanes were calculated by using GraphPad

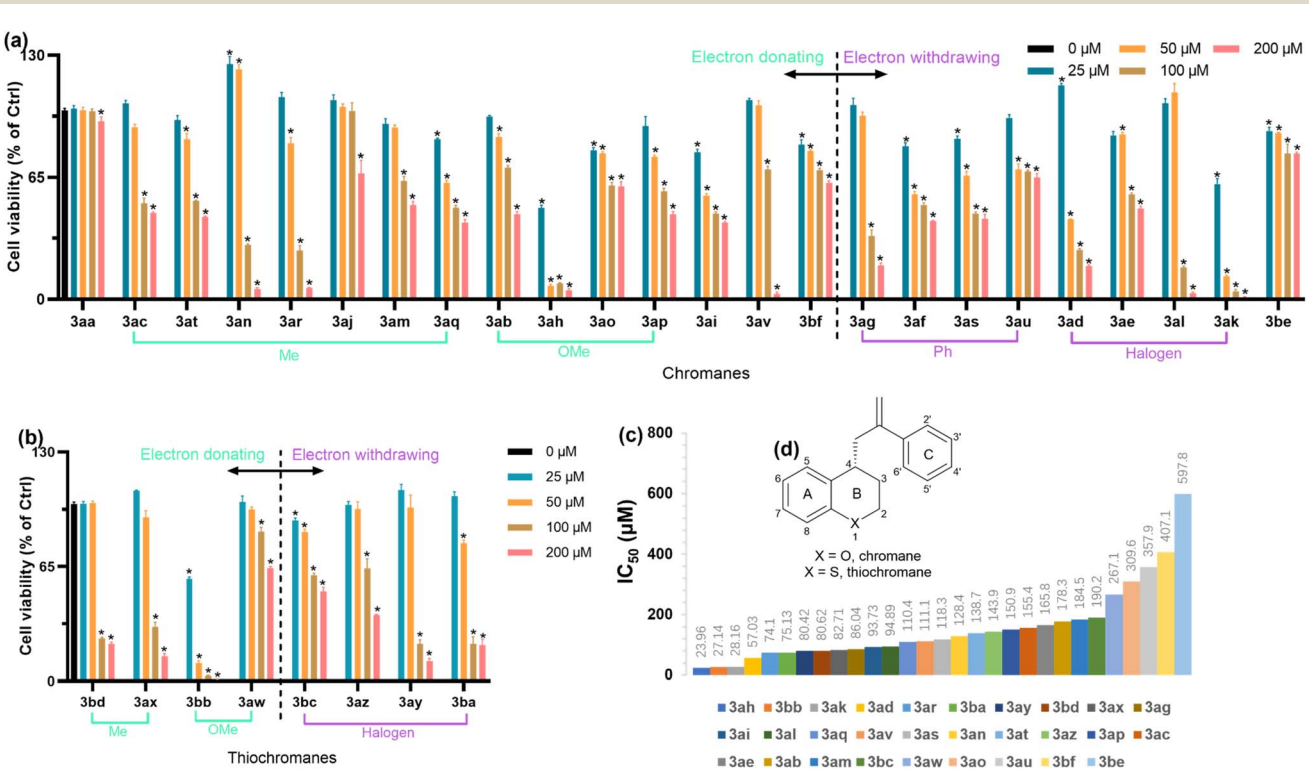

Fig. 3 Cytotoxicity of 4-allyl (thio)chromanes by CCK-8 assay. RAW 264.7 cells were plated in a 96-well plate and treated with each compound (0, 25 μM, 50 μM, 100 μM and 200 μM) for 24 h. The viability of cells was tested by CCK8 assay. (a) The cell viability of RAW 264.7 cells of 4-allyl chromanes **3aa** to **3be**. (b) The cell viability of RAW 264.7 cells of 4-allyl thiochromanes. (c) IC_{50} of (thio)chromanes. (d) The chemical structure of (thio)chromane. Data were expressed as means ± SD from three times independent experiments. (*$p < 0.05$ compared with the control group).

Prism 9.5 (GraphPad Software, San Diego, CA, USA) (Fig. 3(c)). Moreover, we reclassified them into different categories based on the electronic effect of substituents (*i.e.*, electron donating or electron withdrawing), location (*i.e.*, on the A, B, or C ring), and number of substituents (*i.e.*, 1, 2, or 3 substituents) (Fig. 3(d)). Intriguingly, our data implied that: (1) electron-donating or withdrawing groups of 4-allyl chromanes were not critical to the cytotoxicity. (2) Within the methyl-substitute category, *p*-methyl at the C ring (Fig. 3(d)) had lower toxicity than *o*- and *m*-methyl as the IC_{50} was **3an** (*m*-; 128.4 μM) < 166 A (*o*-; 184.5 μM) < **3aj** (*p*-; N. A.); the less the number of C-ring methyl substitutions, the lower the toxicity as evidenced by the IC_{50} of **3ar** (3 methyl; 74.1 μM) < **3aq** (2 methyl; 110.4 μM) < **3aj** (1 methyl; N. A.). (3) Comparing methyl and methoxy substituent, methoxylation might possess lower toxicity than methylation at the A-ring since that IC_{50} of **3ac** (155.4 μM) was lower than **3ab** (178.3 μM). (4) Within the halogen category, Cl-substitution toxicity was lower than Br– and F– as the IC_{50} of **3ad** (–Br at C6 position; 57.03 μM) < **3ae** (–Cl at C6 position; 165.8 μM), **3ak** (–F at C4′ position; 28.16 μM) < **3al** (–Cl at C4′ position; 94.89 μM), and thiochromane **3ba** (–Br at C6 position; 75.13 μM) < **3ay** (–F at C6 position; 80.42 μM) < **3az** (–Cl at C6 position; 143.9 μM). (5) Comparing chromanes and thiochromanes, thiochromanes had lower toxicity in halogen and methoxylation as the IC_{50} of **3al** (chromane, –Cl at C4′ position; 94.89 μM) < **3bc** (thiochromane, –Cl at C4′ position; 190.2 μM), **3ad** (chromane, –Br at C6 position; 57.03 μM) < **3ba** (thiochromane, –Br at C6 position; 75.13 μM), and **3ab** (chromane, –OMe at C6 position; 178.3 μM) < **3aw** (thiochromane, –OMe at C6 position; 267.1 μM). But on the contrary, chromanes had lower toxicity than thiochromanes in methylation as the IC_{50} of **3bd** (thiochromane, –Me at C2′ position; 80.62 μM) < **3am** (chromane, –Me at C2′ position; 184.5 μM) and **3ax** (thiochromane, –Me at C6 position; 82.71 μM) < **3ac** (chromane, –Me at C6 position; 155.4 μM). In summary, our data offered primary indications for further compound synthesis in this field.

3.5. Antioxidative activity of 4-allyl chromanes

Intracellular levels of reactive oxygen species (ROS) are increased in LPS-stimulated RAW 264.7 macrophages[46] and prolonged ROS production is considered to be central to the progression of inflammatory disease.[47] Furthermore, the anti-inflammatory activity of some chromanes (*e.g.*, BL-M) may partly benefit from the antioxidant activity by inhibiting the production of intracellular ROS.[48] Thus, it is important to evaluate the antioxidant activity of our newly developed 4-allyl chromanes by examining the intracellular level of ROS. To assess the antioxidant activity of 4-allyl chromanes, we examined the intracellular level change of ROS by employing a DCFH-DA probe. ROS includes many reactive molecules and free radicals derived from molecular oxygen, which damage DNA and oxidize proteins and lipids (lipid peroxidation). Based on CCK-8 results, the concentration which has no significant

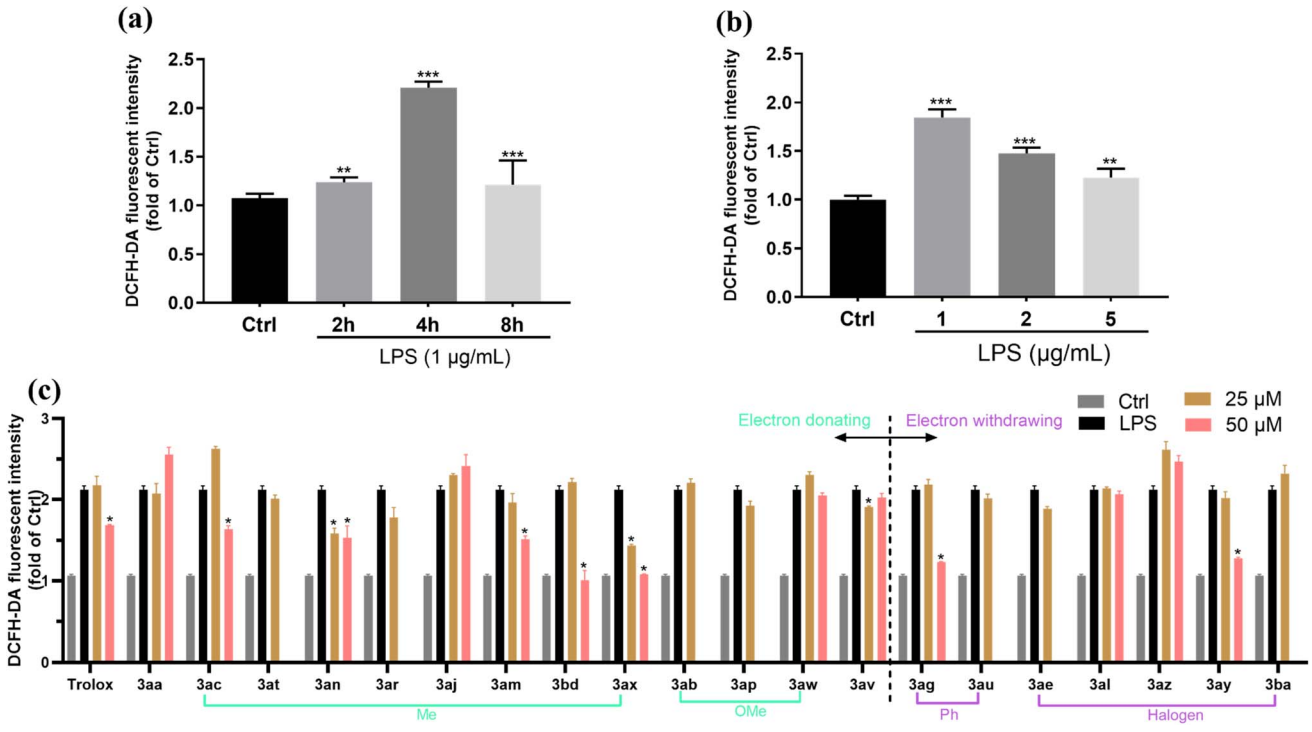

Fig. 4 Antioxidant activity of 4-allyl (thio)chromanes in LPS-induced macrophages. RAW 264.7 cells were plated in a 96-well plate and treated with each compound (0, 25 μM and 50 μM) for 24 h and another 4 h of LPS. Data are presented as folds of DCFH-DA fluorescent intensity compared to control. (a) The concentration (0, 1, 2 and 5 μg mL^{-1}) of LPS on RAW 264.7 cells. (b) Time (2, 4 and 8 h) effects of LPS on RAW 264.7 cells. (c) DCFH-DA fluorescent intensity of 4-allyl (thio)chromanes. Data were expressed as means ± SD from three times independent experiments. (*p < 0.05, **p < 0.01, ***p < 0.001 compared with the control group in (a) and (b); *p < 0.05 compared with the LPS group in (c)).

cytotoxicity of each 4-allyl chromane was chosen for the following experiments. To begin with, the concentration (0–5 μg mL^{-1}) and time (0–8 h) effects of LPS on RAW 264.7 cells were investigated. As shown in Fig. 4(a) and (b), 1 μg mL^{-1} LPS incubated for 4 h exhibited the highest ROS intensity, which were chosen for the following ROS assays. After that, the cells were pre-treated with each 4-allyl chromane for 24 h and then incubated with 1 μg mL^{-1} LPS for 4 h. The data showed that 8 compounds were able to prevent LPS-induced oxidative stress, including **3ac**, **3an**, **3am**, **3bd**, **3ax**, **3av**, **3ag** and **3ay** (Fig. 4(c)). Of note, we found some interesting results: (1) only A- and C-ring substitution were useful. (2) It seemed that methylation was an effective strategy to promote the antioxidant activity of chromanes as 6 out of 9 compounds were methylated. (3) Chiral thiochromanes showed better antioxidant activity potential than its oxygen counterparts. For instance, the ROS inhibition rate of **3ax** (thiochromane, –Me at C6 position) was 32% and 49% at the concentration of 25 μM and 50 μM, whilst it was −24% and 23% in **3ac** (chromane, –Me at C6 position); and the inhibition rate of **3bd** (thiochromane, –Me at C2′ position; 52%) was higher than **3am** (chromane, –Me at C2′ position; 29%) at 50 μM concentration. In addition, we also compared the antioxidant activity of our compounds with Trolox (a lead antioxidant product). The ROS inhibition rate of Trolox was −3% and 20% at 25 and 50 μM, respectively. These observations collectively provide compelling evidence supporting the notion that 4-allyl chromanes might possess appreciable antioxidative ability.

3.6. Anti-inflammatory activity of 4-allyl chromanes

The increased pro-inflammatory cytokines (especially IL-6 and TNF-α) production in RAW 264.7 cells have been reported to play an influential role in the inflammation response.[49] To evaluate the anti-inflammatory effect of these newly synthesized 4-allyl chromanes, TNF-α and IL-6 ELISA kits were employed. Cells were pre-treated with each chromane for 24 h and then stimulation by LPS (1 μg mL^{-1}, 4 h). As shown in Fig. 5(a), 11 chromanes (*i.e.*, **3aa**, **3at**, **3aj**, **3am**, **3bd**, **3ap**, **3au**, **3ae**, **3al**, **3az** and **3ba**) can significantly prevent LPS-indued TNF-α secretion in the macrophages. Another interesting thing is that halogenation at the C6 position obviously prevented TNF-α secretion, but methylation at this position had no effect. This was evidenced by **3ae** (chromane, –Cl at C6 position), **3az** (thiochromane, –Cl at C6 position), **3ba** (thiochromane, –Br at C6 position) and **3ac** (chromane, –Me at C6 position), **3ax** (thiochromane, –Me at C6 position). As shown in Fig. 5(b), only 4 chromanes (*i.e.*, **3aa**, **3al**, **3aj**, and **3aw**) were able to prevent LPS-induced IL-6 secretion. The substitution happened at the C4′ and C6 position, with methyl, methoxy, and chlorine being the substituent group. In summary, **3aa**, **3al** (chromane, –Cl at C4′ position), and **3aj** (chromane, Me at C4′ position) stood out as the most potent inhibitor identified for both pro-inflammatory cytokines. Our data implied the significance of C6 and C4′ substitution on the anti-inflammatory activity. In addition, structure–activity relationship analysis in Fig. 4 and 5 collectively revealed that –Cl or –Me substitution at the C6 or C4′ position might promote the biological potential of 4-allyl

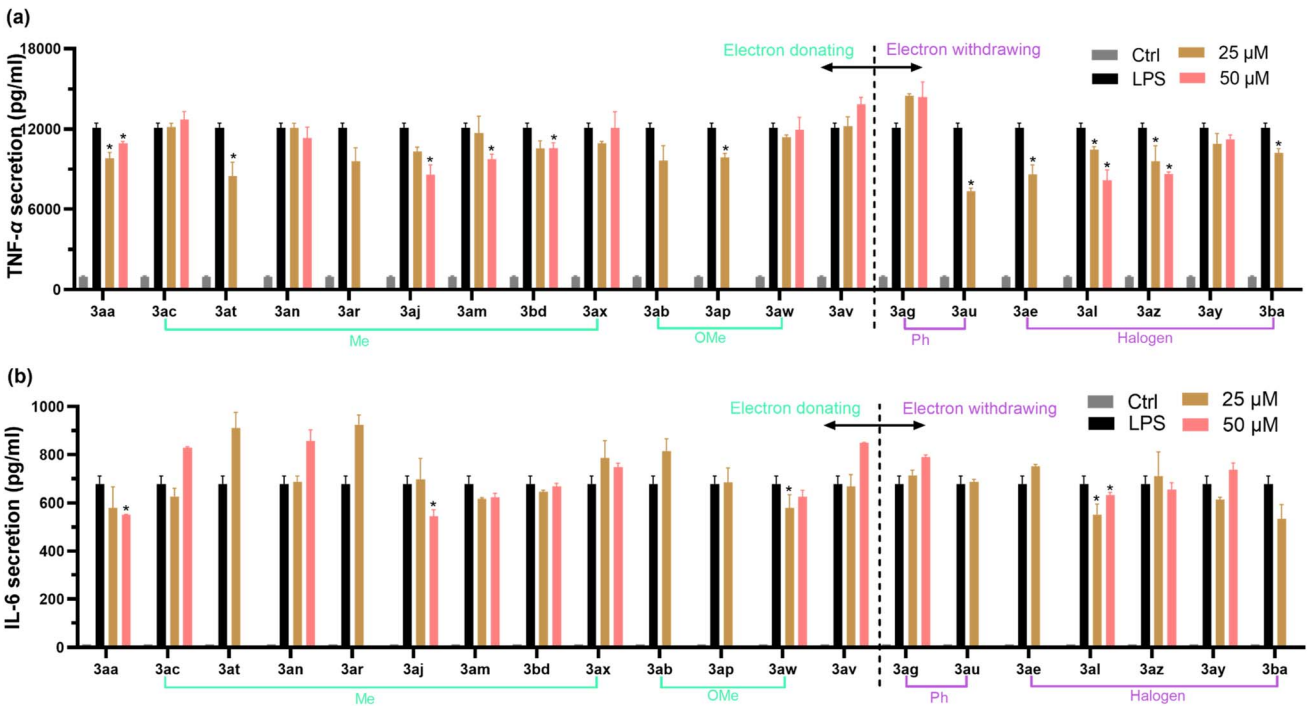

Fig. 5 Anti-inflammatory activity of 4-allyl (thio)chromanes in LPS-induced macrophages. RAW 264.7 cells were plated in a 96-well plate and treated with each compound (0, 25 μM and 50 μM) for 24 h and another 4 h of LPS. The IL-6 and TNF-α secretion in culture supernatants were tested by IL-6 and TNF-α ELISA kits. (a) IL-6 secretion of 4-allyl (thio)chromane compounds. (b) TNF-α secretion of 4-allyl (thio)chromane compounds. Data were expressed as means ± SD from three times independent experiments. (*$p < 0.05$ compared with the LPS group).

chromanes, which offers perspective indications in the designing of novel pharmacological chromanes.

4. Conclusion

In summary, we described an asymmetric synthesis of 4-allyl chromanes through copper(I) hydride-catalyzed hydroallylation of chromene and allylic phosphate electrophiles. A wide range of chiral 4-allyl chromanes was straightforwardly afforded with good yields and extremely high enantioselectivities. They were evaluated for their antioxidative and anti-inflammatory activities in cell model. The data showed that certain 4-allyl chromanes had better antioxidative activity than Trolox and possessed anti-inflammatory ability to reducing the secretion of IL-6 and TNF-α. This makes them a promising class of compounds for further exploration in the development of novel therapies targeting at modulating anti-inflammation. And this led to a final observation that **3aj** (chromane, Me at C4′ position) can ameliorate LPS-stimulated ROS and inflammation with little cytotoxicity. Future work should be contributed to comprehensively unravel the pharmacological application of **3aj**.

Conflicts of interest

The authors declare that there are no conflicts of interest.

Acknowledgements

This work was supported by Shenzhen Science and Technology Program (ZDSYS20220117155800001), Health@InnoHK Initiative Fund of the Hong Kong Special Administrative Region Government (ITC RC/IHK/4/7), and Shenzhen Basic Research Program for Shenzhen Virtual University Park (2021Szvup132). We are grateful for the excellent technical assistance of Ms Dorothy M. C. Chan.

References

1 H. C. Shen, *Tetrahedron*, 2009, **65**, 3931–3952.
2 L. J. Machlin, *α-Tocopherol*, Marcel Dekker, New York, 1980.
3 M. J. Weyant, A. M. Carothers, A. J. Dannenberg, *et al.*, *Cancer Res.*, 2001, **61**, 118–125.
4 K. Y. Chyu, S. M. Babbidge, X. Zhao, *et al.*, *Circulation*, 2004, **109**, 2448–2453.
5 D. Yu, M. Suzuki, L. Xie, *et al.*, *Med. Res. Rev.*, 2003, **23**, 322–345.
6 J. M. Evans, *Chem. Br.*, 1991, **27**, 439–442.
7 M. Sankaran and M. Prasad, *Contraception*, 1974, **9**, 279–289.
8 K. Morito, T. Hirose, J. Kinjo, *et al.*, *Biol. Pharm. Bull.*, 2001, **24**, 351–356.
9 R. T. Thornbury, V. Saini, T. A. Fernandes, *et al.*, *Chem. Sci.*, 2017, **8**, 2890–2897.
10 Y. Ebe, M. Onoda, T. Nishimura, *et al.*, *Angew. Chem., Int. Ed.*, 2017, **56**, 5607–5611.
11 K. Sakamoto and T. Nishimura, *Adv. Synth. Catal.*, 2019, **361**, 2124–2128.
12 Y. Ebe and T. Nishimura, *J. Am. Chem. Soc.*, 2014, **136**, 9284–9287.
13 X. Hao, L. Lin, F. Tan, *et al.*, *Org. Chem. Front.*, 2017, **4**, 1647–1650.
14 H. Ren, X. Y. Song, S. R. Wang, *et al.*, *Org. Lett.*, 2018, **20**, 3858–3861.
15 W. Liu, P. Zhou, J. Lang, *et al.*, *Chem. Commun.*, 2019, **55**, 4479–4482.
16 B. M. Trost, H. C. Shen, L. Dong, *et al.*, *J. Am. Chem. Soc.*, 2003, **125**, 9276–9277.
17 J. S. Cannon, A. C. Olson, L. E. Overman, *et al.*, *J. Org. Chem.*, 2012, **77**, 1961–1973.
18 Q. Liu, K. Wen, Z. Zhang, *et al.*, *Tetrahedron*, 2012, **68**, 5209–5215.
19 U. Uria, C. Vila, M. Y. Lin, *et al.*, *Chem.–Eur. J.*, 2014, **20**, 13913–13917.
20 P. S. Wang, P. Liu, Y. J. Zhai, *et al.*, *J. Am. Chem. Soc.*, 2015, **137**, 12732–12735.
21 P. H. Poulsen, K. S. Feu, B. M. Paz, *et al.*, *Angew. Chem., Int. Ed.*, 2015, **127**, 8321–8325.
22 X. F. Wang, J. An, X. X. Zhang, *et al.*, *Org. Lett.*, 2011, **13**, 808–811.
23 W. Hou, B. Zheng, J. Chen, *et al.*, *Org. Lett.*, 2012, **14**, 2378–2381.
24 Y. Lee and A. H. Hoveyda, *J. Am. Chem. Soc.*, 2009, **131**, 3160–3161.
25 X. Li, C. Wang, J. Song, *et al.*, *J. Org. Chem.*, 2019, **84**, 8638–8645.
26 Q. Yang, Z. Wang, C. H. H. Hor, *et al.*, *Sci. Adv.*, 2022, **8**, eabm9603.
27 Q. Yang, S. Li and J. Wang, *ChemCatChem*, 2020, **12**, 3202–3206.
28 X. Gu, L. Meng, M. Li, *et al.*, *Org. Chem. Front.*, 2021, **8**, 1563–1568.
29 J. Xia, Y. Nie, G. Yang, *et al.*, *Org. Lett.*, 2017, **19**, 4884–4887.
30 Q. Yang, Y. Wang, S. Luo, *et al.*, *Angew. Chem., Int. Ed.*, 2019, **58**, 5343–5347.
31 M. Umeda, K. Sakamoto, T. Nagai, *et al.*, *Chem. Commun.*, 2019, **55**, 11876–11879.
32 Y. M. Wang and S. L. Buchwald, *J. Am. Chem. Soc.*, 2016, **138**, 5024–5027.
33 J. T. Han, W. J. Jang, N. Kim, *et al.*, *J. Am. Chem. Soc.*, 2016, **138**, 15146–15149.
34 J. Lee, S. Torker and A. H. Hoveyda, *Angew. Chem., Int. Ed.*, 2017, **56**, 821–826.
35 Q. F. Xu, X. Zhang and S. L. You, *Org. Lett.*, 2020, **22**, 1530–1534.
36 Q. He, C. M. So, Z. Bian, *et al.*, *Chem.–Asian J.*, 2015, **10**, 540–543.
37 L. Lyu, M. Y. Jin, Q. He, *et al.*, *Org. Biomol. Chem.*, 2016, **14**, 8088–8091.
38 L. Meng and J. Wang, *Synlett*, 2016, **27**, 656–663.
39 D. Xiong, W. Zhou, Z. Lu, *et al.*, *Chem. Commun.*, 2017, **53**, 6844–6847.
40 S. Luo, L. Meng, Q. Yang, *et al.*, *Synlett*, 2018, **29**, 2071–2075.
41 Q. Yang, R. Guo and J. Wang, *Asian J. Org. Chem.*, 2019, **8**, 1742–1765.

42 M. H. Pan, C. S. Lai and C. T. Ho, *Food Funct.*, 2010, **1**, 15–31.
43 M. H. Pan, C. S. Lai, S. Dushenkov, *et al.*, *J. Agric. Food Chem.*, 2009, **57**, 4467–4477.
44 A. García-Lafuente, E. Guillamón, A. Villares, *et al.*, *Inflammation Res.*, 2009, **58**, 537–552.
45 L. I. Mennen, D. Sapinho, A. de Bree, *et al.*, *J. Nutr.*, 2004, **134**, 923–926.
46 M. L. Torres-Rodríguez, E. García-Chávez, M. Berhow, *et al.*, *J. Ethnopharmacol.*, 2016, **188**, 266–274.
47 B. Griffith, S. Pendyala, L. Hecker, *et al.*, *Antioxid. Redox Signaling*, 2009, **11**, 2505–2516.
48 M. Moniruzzaman, G. Lee, S. Bose, *et al.*, *Biol. Pharm. Bull.*, 2015, **38**, 1831–1835.
49 L. Dong, L. Yin, Y. Zhang, *et al.*, Anti-inflammatory effects of ononin on lipopolysaccharide-stimulated RAW 264.7 cells, *Mol. Immunol.*, 2017, **83**, 46–51.